Journal of Chemistry and Technologies, 2024, *32*(4), 932-938

Journal of Chemistry and Technologies

pISSN 2663-2934 (Print), ISSN 2663-2942 (Online).

journal homepage: http://chemistry.dnu.dp.ua
editorial e-mail: chem.dnu@gmail.com

UDC 661.183.6:[54.057+544.02](045)

EFFECT OF SYNTHESIS TIME ON THE MORPHOLOGY OF MONODISPERSE SILICA MICROSPHERES

Junjie Yu, Antonina I. Bondarieva, Viktoriia Yu. Tobilko*

National Technical University of Ukraine "Igor Sikorsky Kyiv Polytechnic Institute", 37 Beresteiskyi Ave., Kyiv, 03056, Ukraine

Received 14 November 2024; accepted 2 December 2024; available online 25 January 2025

Abstract

Silica (SiO_2) microspheres can be used in pharmaceutical, cosmetic, food, coating and other technological applications. Consequently, the task is to search for optimal parameters for easy synthesis of monodisperse silica microspheres with controlled structural and physicochemical characteristics. The aim was to study the effect of synthesis time on the formation of silica microspheres for control of their surface morphological properties. The synthesis was conducted by alkaline hydrolysis in an aqueous/alcohol solution using structure-directing agents, namely cetyltrimethylammonium bromide (CTAB) and sodium salicylate (NaSal), in conjunction with an inorganic precursor, namely tetraethoxysilane (TEOS). The synthesis time varied from 1.5 to 5 hours. The following methods were used to study the synthesised silica microspheres: X-ray powder diffraction (XRD), Fourier-transform infrared spectroscopy (FTIR), scanning electron microscopy (SEM) and low-temperature N_2 adsorption/desorption method. As a result were synthesized silica spheres with a consistent diameter of approximately 200 nm and mesoporous structure, regardless of synthesis duration. However, the thickness of the nanosheets forming the sphere structure increased from 7 nm to 22 nm as the synthesis time extended. The sample synthesised for 1.5 hours showed the highest specific surface area, reaching 504 m^2/g.

Keywords: silica; sol-gel; porous structure; mesopores; dendritic nanoparticles; synthesis.

ВПЛИВ ЧАСУ СИНТЕЗУ НА МОРФОЛОГІЮ МОНОДИСПЕРСНИХ МІКРОСФЕР КРЕМНЕЗЕМУ

Цзюньцзе Юй, Антоніна І. Бондарєва, Вікторія Ю. Тобілко

Національний технічний університет України «Київський політехнічний інститут імені Ігоря Сікорського», просп. Берестейський, 37, Київ, 03056, Україна

Анотація

Мікросфери діоксиду кремнію (SiO_2) можуть бути використані в фармацевтичній, косметичній, харчовій галузях, виробництві покриттів та інших технологічних процесах. Тому, важливим завданням є пошук оптимальних параметрів для легкого синтезу монодисперсних мікросфер кремнезему з контрольованою структурою та фізико-хімічними характеристиками. Метою роботи було вивчення впливу часу синтезу на формування мікросфер кремнезему для контролю морфологічних властивостей їх поверхні. Синтез проводили методом лужного гідролізу в водно-спиртовому розчині із використанням структуроутворюючих агентів, а саме цетилтриметиламоній броміду (ЦТАБ) та натрій саліцилату (NaSal), у поєднанні з неорганічним прекурсором, а саме тетраетоксисиланом (ТЕОС). Тривалість синтезу варіювалась від 1.5 до 5 годин. Для дослідження синтезованих мікросфер кремнезему застосовували такі методи: рентгенофазовий аналіз (РФА), інфрачервона спектроскопія з Фур'є перетворенням (ІЧ-спектроскопія), скануюча електронна мікроскопія (СЕМ) і метод низькотемпературної адсорбції/десорбції азоту. В результаті були синтезовані мікросфери діоксиду кремнію з постійним діаметром близько 200 нм та мезопористою структурою, незалежно від тривалості синтезу. Однак, зі збільшенням часу синтезу товщина наношарів, що формують структуру сфери, зростала від 7 нм до 22 нм. Зразок, синтезований впродовж 1.5 години, показав найвищу питому поверхню, яка досягла 504 $м^2/г$.

Ключові слова: кремнезем; золь-гель; пориста структура; мезопори; дендритні наночасточки; синтез.

**Corresponding author: e-mail: v.tobilko@kpi.ua*

doi: 10.15421/jchemtech.v32i4.315165

Journal of Chemistry and Technologies, 2024, *32*(4), 932-938

Introduction

In recent years, there has been a notable increase in interest from both industry and scientific research communities in using of porous solids with ordered structures, with silica being the most common [1–4]. This is due to the growing number of their potential uses in fields such as pharmaceutics, cosmetics, food, coating industries etc. [5–7]. Consequently, there is an ever-increasing requirement for the development of silica porous materials with varying dimensions, surface areas, pore sizes and morphologies.

The use of silica as a porous material is well established, largely due to the properties that it offers, including a low density, low toxicity, good biocompatibility, ease of surface modification, stability, and cost effectiveness. The discovery of the Stöber method [8] for the synthesis of monodisperse silica, work by Kresge on the template-directed synthesis of mesoporous silica (such as MCM-41) [9] and work by researchers at the university of California Santa Barbra [10] on the triblock co-polymer templated synthesis of mesoporous silica (SBA-15) constituted the initial point of investigation into the potential for synthesising a variety of mesoporous and nanosilica materials.

In 2010, a novel class of high-surface-area silica nanospheres with a unique open central–radial structures, has been synthesized [11]. The specific characteristics of those materials are primarily attributable to their distinctive dendritic fibrous morphology, which is essentially accessible from all sides. This contrasts with the tubular pores observed in MCM-41 and SBA-15. In addition, the main disadvantages identified in the practical application of materials of the structural type such as MSM-41 and SBA-15 are their poor solubility in solvents (due to particle size), and low temperature stability (the thinsilica walls are prone to break down to heated at high temperatures).

The majority of potential sphere applications require the specific functional properties and characteristics of porous silica materials, such as material particle size with narrow range distribution. This fact causes the demand to search for optimal parameters synthesis of monodisperse silica microspheres with control structural and physicochemical characteristics. Existing techniques include variation of temperature, type of inorganic precursor and catalyst, solvent content, as well as the reaction time. An approach of varying the dielectric constants of the reaction media using different water miscible alcohols has also been described, resulting in a decrease in particle size as the polarity of the media decreases [12; 13]. A group of researchers has shown that variation of the Hansen solubility parameters of the reaction media is an effective instrument for adjusting particle size and distribution [14].

The effect of synthesis time on the morphology of porous silica microspheres synthesised via the water-in-oil emulsion-mediated sol-gel method between 24 and 72 hours was the subject of investigation in [15]. The longer synthesis time resulted in denser silica spheres with decreased pore sizes.

In work [16], the authors studied the impact of co-solvents on the regulation of the structure of dentritic mesoporous silica nanoparticles (DMSN), in particular, the change in structure as a function of time. When ethanol is used as a solvent, the time period of the structural transformation from DMSN large pores to mesoporous silica nanoparticles (MSN) with small pores decreases with an increase in the amount of ethanol used in the synthesis. Nevertheless, despite the variation in the volume of ethanol employed in the synthesis, with the reaction time varying from 15 minutes to 2 hours, the structure of the large-pore DMSNs underwent a gradual transformation to that of the small-pore MSNs.

The autors [17] also report about unique dynamic structural transition from large-pore DMSN with a dahlia-like morphology to pomegranate-like MSN with small mesopores.

It is important to note that the above works present a variety of options for the synthesis of monodispersed silica microspheres using cetyltrimethylammonium bromide (CTAB) and tetraethoxysilane (TEOS) as a basis components. It is for this reason that the task of identifying the most effective method for the production of porous materials based on silica remains a pertinent one.

Material and Methods

Chemical and reagents

The following chemical and reagents were used in this work: cetyltrimethylammonium bromide (CTAB) and sodium salicylate (NaSal) as structure-directing agents, tetraethoxysilane (TEOS) as inorganic precursor, and triethanolamine (TEA) as a catalyst were purchased from Merck. Distilled water and ethanol (EtOH) were used as solvents. All chemicals were in analytic grade and used without further purification.

Methods for preparation of silica microspheres

Journal of Chemistry and Technologies, 2024, *32*(4), 932-938

The material were synthesized by one-plot method according to a modified method described in [18–20]. In the first stage, 1.36 g of TEA were dissolved in a 500 ml of distilled water. The solution obtained should be placed in a water bath set at 80 °C with uniform stirring for a period of 30 minutes. Subsequently, 7.6 g of CTAB and 3.36 g of NaSal should be added to the system, and stirring should continue for an additional hour. Concurrently, a solution comprising 80 ml of TEOS and 10ml of ethanol should be prepared and introduced to the mixture via peristaltic pump over a period of 30 minutes, with constant stirring. After that, the mixture was continuously stirred for a further 90 minutes at 80 °C. Then, the solid phase is separated from the liquid phase by centrifugation and washed three times with a mixture of water and ethanol. The resulting precipitate is then calcined at 550 °C for a period of 6 hours. The obtained sample is coded SiO_2-1.5. The additional two samples were synthesised in a methodology analogous to that described above, with the stirring time increased from 90 minutes to 180 minutes and 300 minutes. Accordingly, these samples are coded SiO_2-3 and SiO_2-5, respectively. The general synthesis steps are shown in Fig. 1.

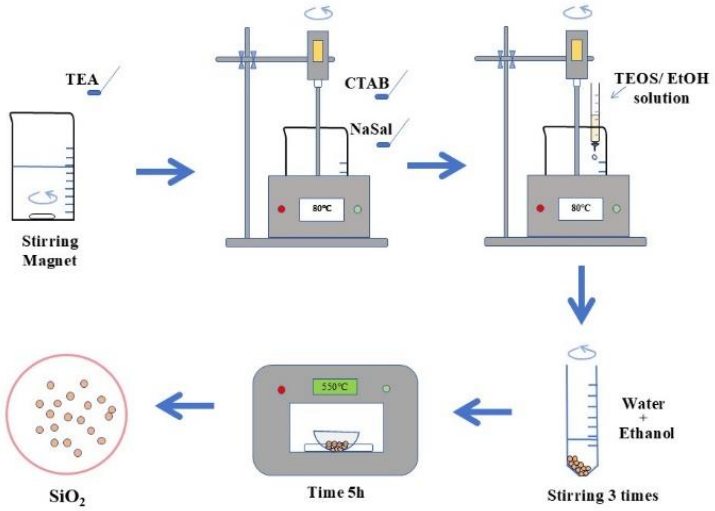

Fig. 1. Synthesis steps of silica microspheres

Characterization and analytic methods

X-ray powder diffraction (XRD) of the prepared silica microspheres were recorded on D8 AdvanceX diffractometer (Germany) under the following conditions: range of 10–80^0 (2θ) using CuKα radiation. The crystal structure of the materials was determined based on the peak shape and position of the tested materials. The crystal structure of the samples was analyzed using the JCPDS Database (International Center for Diffraction Data).

Fourier-transform infrared spectroscopy (FTIR) was used to identify the functional groups and gather relevant information about the silica materials. The prepared materials were subjected to testing using a Bruker Vertex 70 (Germany) model infrared spectrometer with a swept range of 500–4000 cm^{-1}.

The morphology of SiO_2 samples was studied using scanning electron microscopy (SEM) on a field-emission scanning electron microscope Nova Nano SEM450 (USA).

The porous structure parameters were determined on evacuated samples by the low-temperature N_2 adsorption/desorption method (Quantachrome NOVA-2200e Surface Area and Pore Size Analyzer, USA). Processing of the obtained data was carried out using the ASiQwin software. The value of the specific surface area (S_{BET}, m^2/g) was calculated by the multipoint BET method (Brunauer, Emmett and Teller), and the external pore surface (S_{ext}, m^2/g) and micropore surface (S_{micro}, m^2/g) were estimated by the t-method. The total pore volume (V_Σ, cm^3/g) was determined using the maximum adsorbed volume of nitrogen at a relative pressure $p/p_o \approx 1$. The volume of micropores (V_{micro}, cm^3/g) was estimated by the t-method, and their percentage content (W_{micro}, %) was calculated using the Eq.1:

$$W_{micro} = \frac{V_{micro}}{V_\Sigma} \cdot 100 \qquad (1)$$

The distribution of pore size was measured by BJH (Barrett-Joyner-Halenda) model. The average pore radius (R, nm) was calculated using the Eq.2:

Journal of Chemistry and Technologies, 2024, *32*(4), 932-938

$$R = \frac{2V_{\Sigma}}{S_{BET}} \quad (2)$$

Results and Discussion

In order to investigate the impact of synthesis time on the morphology and structural properties of the synthesised silica microspheres, a series of studies were conducted.

The analysis of the obtained samples diffractograms (Fig. 2) revealed the presence of a single, broad diffraction peak at 2θ = 22^0, indicative of amorphous silica (JCPDS card No. 29-0085).

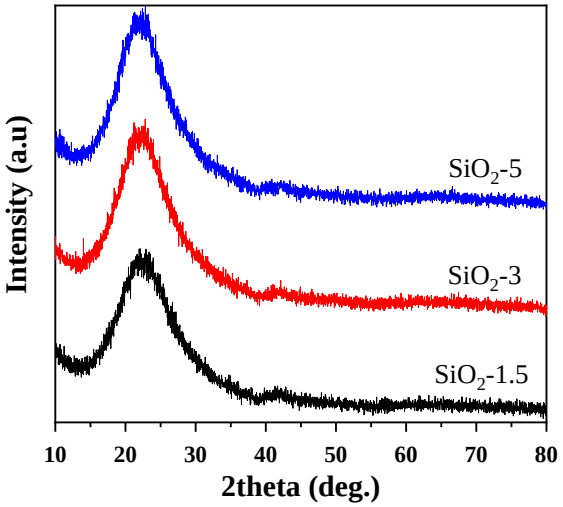

Fig. 2. XRD difftaction patterns of synthesis silica materials

The analysis of structural features using infrared spectroscopy (Fig. 3) revealed that all samples exhibited a wide peak at 3433 cm^{-1}, which was identified as the antisymmetric stretching vibration peak of -OH group. The peak located at 1640 cm^{-1} was attributed to the bending vibrations of the water molecule [21]. Nevertheless, the intensity of these peaks is greatest for the SiO_2-1.5 sample. This results from the fact that the calcination process produces a discontinuity in the dehydroxylation process. Once the hydrophobic surfactant molecules have been completely removed, the large surface area is then covered by silanol species, which immediately adsorb molecular water [21; 22]. The strong and wide band observed at 1093 cm^{-1} is attributed to the Si-O-Si antisymmetric stretching vibration. The peak observed at 966 cm^{-1} is attributed to the Si-O vibration bond of isolated Si-OH groups. The peak at 803 cm^{-1} is identified as the symmetric stretching vibration of the O-Si-O bond. Accordingly, the samples contain all the vibrational bands of Si-OH, O-Si-O and Si-O-Si, which are characteristic of amorphous SiO_2 [23; 24].

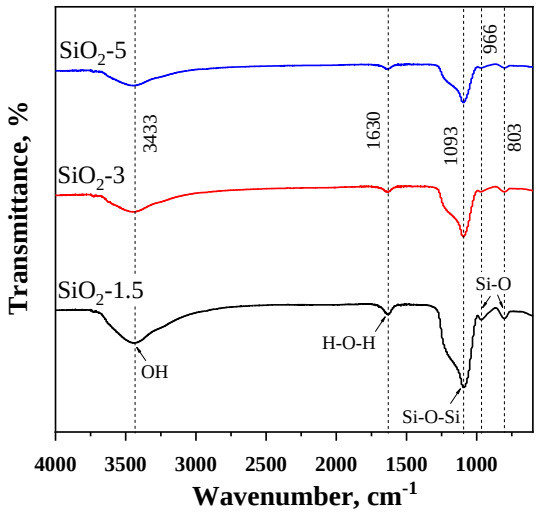

Fig. 3. IR-spectra of synthesis silica materials

The morphology of silica is of critical importance in determining its properties and potential applications. The images obtained via scanning electron microscopy (Fig. 4) that silica microspheres, when subjected to varying reaction times, exhibit monodisperse spheres with a diameter of approximately 200 nm and evident pores. As illustrated in Fig. 4(a, b), the spherical silica material subjected to a reaction time of 1.5 hours shows a nanoscale edge of approximately 7 nm and distinct mesopores. Furthermore, the high-magnification SEM image (Fig. 4a) reveals a substantial internal space within the silica spheres with acute edges. The spheres are observed to be isolated from one another, lacking any apparent bonding, which may facilitate the creation of a larger reaction area and the occurrence of specific reactions.

As illustrated in Fig. 4 (c, d), the reaction time of 3 hours results in a transformation of the silica spheres' edges from thin nanosheets to thicker strip-like edges. In particular, the dimensions of these edge nanosheets increase from 7 nm to 16 nm. Nevertheless, the edge shape and growth trend can still be discerned from the high-magnification SEM in Fig. 4(c), indicating that it evolved from a thin edge. This indicates that with an extended reaction time, the silica material continues to expand in the lateral direction rather than the longitudinal one. It is noteworthy that this change occurs solely in the thickness of the edges while the overall morphology with a 200 nm diameter is maintained.

Journal of Chemistry and Technologies, 2024, *32*(4), 932-938

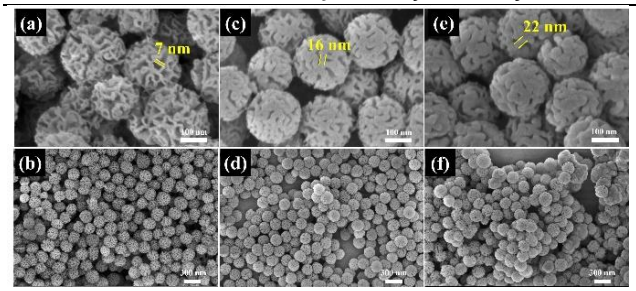

Fig. 4. SEM images of silica microspheres (a, b – SiO_2-1.5; c, d – SiO_2-3; e,f – SiO_2-5)

Upon reaching a reaction time of five hours (Fig. 4e), while the overall size and morphology of the SiO_2-5 material remain relatively consistent, exhibiting a spherical form with a porous structure, the edge widths continue to thicken, reaching up to 22 nm. At this juncture, the edges of the spherical silica are constituted entirely of nanostrips, and the presence of sharp edges is no longer discernible. At low magnification, as illustrated in Fig. 4(f), the material begins to exhibit localized lumping or stacking. Consequently, a portion of the material loses its monodisperse nature, which leads us to conclude that further prolonging the reaction time is unnecessary.

The general principle of synthesis can be described as follows. In aqueous systems with CTAB and NaSal, the application of salicylate anion is role of form large pores, due to its superior micelle penetration effect. In particular, the strong electrostatic attraction and high miscibility of NaSal and CTAB result in a highly favourable interaction energetically. Sal^- anions ultimately migrate into CTA^+ micelles, with their hydrophobic portions inserted into the hydrophobic regions of the micelles. This results in an increase in the packing parameter, which induces a structural transition in the CTA^+ micelles from spherical to vesicular or lamellar, and subsequently to central radial [25]. An increase in the reaction time from 1.5 hours to 5 hours results in a slowing of the process, although it does not reach a complete halt.

The process of wall thickening of synthesised SiO_2 particles affects the overall textural parameters of the particles, including specific surface area, pore size and pore volume. As illustrated in Fig. 5, all samples of SiO_2 microspheres exhibited isotherms of low temperature nitrogen adsorption/desorption belong to the type IV isotherms with H3-type hysteresis loops according to the IUPAC classification. The nature of the hysteresis loop allows us to ascertain that the porous structure of all samples is constituted by spherical particles of homogeneous size, which is the same as commercial highpurity grade silica gel [2]. This type of isotherms is typical for materials with a mesoporous structure.

However, in comparison with the industrial silica sample, which exhibits a relatively narrow pore size distribution concentrated around 2.5–3 nm [2], the obtained samples (SiO_2-1.5; SiO_2-3; SiO_2-5) display a considerably wider pore size distribution (Fig.6). The pore sizes of all SiO_2 microspheres range from approximately 5 to 50 nm.

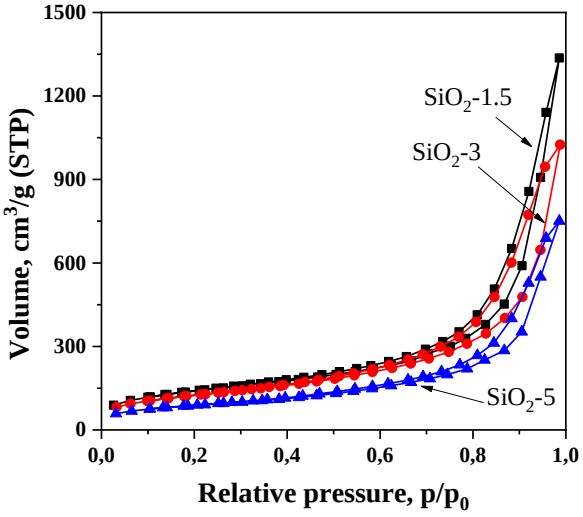

Fig. 5. Isotherms of low-temperature N_2 adsorption/desorption of the synthesis SiO_2

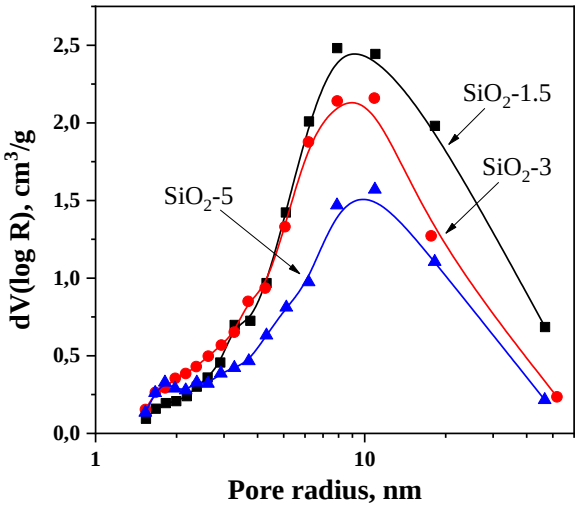

Fig. 6. Pore size distribution by radius of the synthesis SiO_2

The parameters of the porous structure of the investigated samples are presented in Table. As the synthesis time is increases, the specific surface area of the samples shows a gradual decrease of approximately 2 times. Concurrently, the total pore volume is observed to diminish. Among the synthesised samples, the SiO_2-1.5 sample is the

only one to show a microporous structure in addition to meso-structures.

Table

Parameters of the porous structure of SiO_2 samples

Sample	S_{BET}, m^2/g	S_{ext}, m^2/g	S_{micro}, m^2/g	V_{Σ}, cm^3/g	V_{micro}, cm^3/g	V_{micro}, %	R, nm
SiO_2-1.5	504	448	56	2.067	0.017	0.8	8.2
SiO_2-3	452	452	-	1.586	-	-	7.02
SiO_2-5	308	308	-	1.161	-	-	7.5

This effect due to the continued growth of the outer edges, thickening, and extrusion of the original pore space, that observation aligns with SEM images (Fig. 4).

Conclusions

The analysis conducted via XRD and FTIR corroborated the amorphous nature of the synthesised SiO_2 and the presence of characteristic Si-OH, O-Si-O, and Si-O-Si bands, which are indicative of amorphous silica structures. The IR-spectroscopy analysis demonstrated that shorter synthesis times resulted in incomplete hydrolysis of TEOS, as evidenced by the presence of free Si-OH groups in the SiO_2 -1.5 sample.

Across the full range of synthesis times, the diameter of the silica microspheres remained at approximately 200 nm. However, the edges of the nanosheets exhibited a gradual thickening as synthesis time was extended, increasing in width from 7 nm at 1.5 hours to 22 nm at 5 hours. This edge thickening affected the overall texture of the samples.

All samples exhibited mesoporous structures with type IV isotherms and H3 hysteresis loops, indicative of uniform spherical particles with a wide range of pore sizes. The SiO_2-1.5 sample demonstrated the highest specific surface area (504 m^2/g) and contained both mesoporous and microporous structures. With longer synthesis times, the specific surface area decreased as a result of pore space reduction caused by the thickening of the nanosheets.

The study revealed that a synthesis time of 1.5 hours is optimal for achieving a high specific surface area and morphology without significant pore coalescence or edge thickening. Prolonged synthesis times (up to 5 hours) resulted in the formation of materials with reduced surface area, pore volume, and aggregation of individual particles SiO_2.

The results obtained show the effect of synthesis time on nanosheet thickness and specific surface area, thereby providing insights into the optimisation of the structural properties of silica spheres for potential applications in catalysis, adsorption, and material science.

References

[1] Kurbanov, M., Tulaganov, S., Nuraliev, U., Andriyko, L., Goncharuk, O., Guzenko, N., Nychyporuk, Yu., Marynin, A. (2023). Comparative characteristics of the structure and physicochemical properties of silica synthesized by pyrogenic and fluoride methods. *Silicon*, 15, 1221–1233. https://doi.org/10.1007/s12633-022-02087-7

[2] Yu, J., Bondarieva, A., Tobilko, V., Pavlenko, V. (2023). Adsorption removal of Cu(II) using Ni-modified silica gel. *Water and Water Purification Technologies. Scientific and Technical News, 37*(3), 3–12. https://doi.org/10.20535/2218-930032023302423

[3] Szczęśniak, B., Choma, J., Jaroniec, M. (2020). Major advances in the development of ordered mesoporous materials. *Chemical Communications*, *56*, 7836–7848. https://doi.org/10.1039/D0CC02840A

[4] Usman, P., Duru, I.A., Akalezi, C.O., Njoku, C., Kovo, A., Oguzie, E.E. (2024). Mesoporous silica-based smart nanocontainers for corrosion inhibition: a mini-review. *Journal of Coatings Technology and Research*. https://doi.org/10.1007/s11998-024-00942-3

[5] Zhang, S., Bai, J., Kong, W., Song, H., Liu, Yu., Liu, G., Ma, Li., Zhou, L., Jiang, Y. (2024). Dendritic mesoporous silica nanoparticles for enzyme immobilization. *Green Chemical Engineering*, *5*(2), 173–186. https://doi.org/10.1016/j.gce.2023.07.002

[6] Polshettiwar, V. (2022). Dendritic fibrous nanosilica: discovery, synthesis, formation mechanism, catalysis, and CO_2 capture-concersion. *Accounts of Chemical Research, 55*(10), 1395–1410. https://doi.org/10.1021/acs.accounts.2c00031

[7] Sharma, K., Hooda, A., Goyat, M.S., Rai, R., Mittal, A. (2022). A review on challenges, recent progress and applications of silica nanoparticles based superhydrophobic coatingds. *Ceramic International*, *48*(5), 5922–5938. https://doi.org/10.1016/j.ceramint.2021.11.239

[8] Stöber, W., Fink, A., Bohn, E. (1968). Controlled growth of monodisperse silica spheres in the micron size range. *Journal of Colloid and Interface Science*, *26*(1), 62–69. https://doi.org/10.1016/0021-9797(68)90272-5

[9] Kresge, C.T., Roth, W.J. (2013). The discovery of mesoporous molecular sieves from the twenty year perspective. *Chemical Society Reviews*, *42*(9), 3663–3670. https://doi.org/10.1039/C3CS60016E

[10] Rahmat, N., Abdullah, A., Mohamed, A. (2010). A review: mesoporous Santa Barbara Amorphous-15, types, synthesis and its applications towards biorefinery production. *American Journal of Applied Sciences*, *7*(12), 1579–1586. https://doi.org/10.3844/ajassp.2010.1579.1586

[11] Polshettiwar, V., Cha, D., Zhang, X., Basset, J.M. (2010). High-surface-area silica nanospheres (KCC-1) with a fibrous morphology. *Angewandte Chemie, 49*(50), 9652–9656. https://doi.org/10.1002/anie.201003451

[12] Wang, X.-D., Shen, Z.-X., Sang, T., Cheng, X.-B., Li, M.-F., Chen, L.-Y., Wang, Z.-S. (2010). Preparation of spherical silica particles by Stöber process with high concentration of tetra-ethyl-orthosilicate. *Journal of Colloid and Interface Science*, 341(1), 23-29. https://doi.org/10.1016/j.jcis.2009.09.018

[13] Lee, K., Sathyagal, A.N., McCormick, A.V. (1998). A closer look at an aggregation model of the Stöber process. *Colloids and Surfaces A: Physicochemical and Engineering Aspects*, *144*(1-3), 115–125. https://doi.org/10.1016/S0927-7757(98)00566-4

[14] Sivolapov, P., Myronyuk, O., Baklan, D. (2022). Synthesis of Stober silica nanoparticles in solvent environments with different Hansen solubility parameters. *Inorganic Chemistry Communications*, 143, 109769. https://doi.org/10.1016/j.inoche.2022.109769

[15] Chen, Q., Larismaa, J., Keski-Honkola, A., Vilonen, K., Söderberg, O., Hannula, S.-P. (2012). Effect of synthesis time on morphology of hollow porous silica microspheres. *Materials Science*, *18*(1), 66–71. http://dx.doi.org/10.5755/j01.ms.18.1.1344

[16] Feng, J., Liu, Y., Liu Ch., Hu, W., Zhang, Ch., Li, S., Song, Y., Yu, Ch. (2020). The impact of ethanol and chlorobenzene in the structure regulation of dendritic mesoporous silica nanoparticles. *Microporous and Mesoporous Materials*, 307, 110504. https://doi.org/10.1016/j.micromeso.2020.110504

[17] Wang, Yu., Song, H., Yang, Y., Liu, Y., Tang, J., Yu, Ch. (2018). Kinetically controlled dendritic mesoporous silica nanoparticles: from dahlia- to pomegranate-like structures by micelle filling. *Chemistry of Materials*, *30*(16), 5770–5776. https://doi.org/10.1021/acs.chemmater.8b02712

[18] Yu, J., Tobilko, V. (2024). Adsorption removal of copper(II) from water by zero valent iron loaded dendritic mesoporous silica. *Technology Audit and Production Reserves, 5*(3(79), 6–12. https://doi.org/10.15587/2706-5448.2024.314231

[19] Zhang, K., Xu, L.-L., Jiang, J.-G., Calin, N., Lam, K.-F., Zhang, S.-J., Wu, H.-H., Wu, G.-D., Albela, B., Bonneviot, L., Wu, P. (2013). Facile large-scale synthesis of monodisperse mesoporous silica nanospheres with tunable pore structure. *Journal of the American Chemical Society*, *135*(7), 2427–2430. https://doi.org/10.1021/ja3116873

[20] Gao, F., Lei, Ch., Liu, Y., Song, H., Kong, Y., Wan, J., Yu, C. (2021). Rational design of dendritic mesoporous silica nanoparticles' surface chemistry for quantum dot enrichment and an ultrasensitive lateral flow immunoassay. *ACS Applied Materials & Interfaces*, *13*(18), 21507–21515. https://doi.org/10.1021/acsami.1c02149

[21] Innocenzi, P., Falcaro, P., Grosso, D., Babonneau, F. (2003). Order-disorder transitions and evolution of silica structure in self-assembled mesostructured silica films studied through FTIR spectroscopy. *The Journal of Physical Chemistry B*, *107*(20), 4711–4717. https://doi.org/10.1021/jp026609z

[22] Lei, Z., Pang, X., Li, Na, Lin, L., Li, Y. (2009). A novel two-step modifying process for preparation of chitosan-coated Fe_3O_4/SiO_2 microspheres. *Journal of Materials Processing Technology*, *209*(7), 3218–3225. https://doi.org/10.1016/j.jmatprotec.2008.07.044

[23] Dong, K., Wu, S., Chang, B., Sun, T. (2023). Zero-valent iron supported by dendritic mesoporous silica nanoparticles to purify dye wastewater. *Journal of Environmental Chemical Engineering*, *11*(5), 110434. https://doi.org/10.1016/j.jece.2023.110434

[24] Li, H., Si, R., Wang, W., Huang, Y., Xiang, M., Wang, C., Chen, S., Cao, W., Lu, Z., Huang, M. (2021). Sulfidated nanoscale zero-valent iron dispersed in dendritic mesoporous silica nanospheres for degrading tetrabromobisphenol A. *Colloids and Surfaces A: Physicochemical and Engineering Aspects*, 621, 126586. https://doi.org/10.1016/j.colsurfa.2021.126586

[25] Yang, Y., Bernardi, S., Song, H., Zhang, J., Yu, M., Reid, J.C., Strounina, E., Searles, D.J., Yu, C. (2016). Anion assisted synthesis of large pore hollow dendritic mesoporous organosilica nanoparticles: understanding the composition gradient. *Chemistry of Materials*, *28*(3), 704–707. https://doi.org/10.1021/acs.chemmater.5b03963